Computational Investigation of the Weakly Bound Dimers HOX···SO_3 (X = F, Cl, Br)

Mohammad Solimannejad*

Quantum Chemistry Group, Department of Chemistry, Arak University, 38156−879 Arak, Iran

Ljupčo Pejov

Institute of Chemistry, Arhimedova 5, PO Box 162, 1000 Skopje, Republic of Macedonia

Received: June 19, 2004; In Final Form: October 12, 2004

The electronic structure and thermochemical stability of the HOX−SO_3 (X = F, Cl, Br) complexes is studied using second-order Møller−Plesset perturbation theory (MP2). The calculated dissociation energies of the HOF−SO_3, HOCl−SO_3, and HOBr−SO_3 complexes are 5.43, 6.02, and 5.98 kcal mol^{-1} at MP2/6-311++G(3df,3pd) level, respectively. *Anharmonic* OH stretching frequencies of the HOX (X = F, Cl, Br) moieties along with the frequency shifts upon complex formation are calculated at the MP2/6-311++G(2df,2p) level. AIM and NBO analyses were also performed. Theoretical data strongly encourage performing of matrix-isolation studies of the title complexes and their spectroscopic identification.

Introduction

The substantial importance of noncovalent intermolecular interactions in practically all areas of contemporary chemical physics has been demonstrated in a number of studies of such systems.[1] From a fundamental point of view, the "van der Waals molecules" formed by the noncovalent interactions are significant in their own right, as they bridge the gap between the free molecular systems and the corresponding condensed phases they form. From purely applicative aspect, the noncovalently bonded molecular clusters are of certain practical importance in many areas of applied science, such as atmospheric chemistry and catalysis, as well as in biochemically relevant processes. A rather illustrative example related to the significance of noncovalent systems in atmospheric chemistry is that the proposed mechanisms aiming to explain the ozone layer depletion involve formation of certain intermolecular complexes (or clusters).[2−5] To be able to understand the details of the reactions occurring in atmospheric conditions, one should be first of all capable of understanding the structure, stability and some other properties of the intermolecular clusters taking part in these reactions. It is thus of certain interest to study such noncovalently bonded clusters in controlled laboratory conditions. However, understanding of the structures and other relevant binding properties of such clusters on a fundamental level requires a close cooperation between the most sophisticated experimental and theoretical approaches. In most cases, the experimental detection of the existence of a particular intermolecular interaction is based on indirect spectroscopic data. Thus, besides the more thorough theoretical basis for the interpretation of spectroscopic manifestations of the intermolecular interactions which are crucial for detection of the clusters in question, contemporary theoretical methods may also initiate experimental searches for particular complexes or clusters which have not been previously studied, by providing relevant theoretical data for the thermodynamical stability and the various spectroscopic (e.g., vibrational) properties of the interactions/complexes. It is the second advantage of theoretical methodologies that this paper is devoted to.

Continuing our previous studies of various intermolecular interactions,[6−10] in the present study, we focus on the possibility of formation of the complexes such as HOX···SO_3 (X = F, Cl, and Br) in the atmosphere. The noncovalently bonded complexes of HOX (X = F, Cl, Br) with SO_3 are expected to be of prime importance for atmospheric chemistry, as some other complexes involving SO_3 molecule have been shown to be of particular relevance to the catalytic ozone removal processes. Bearing in mind that the HOX species (where X is F, Cl or Br) could be easily formed in the atmosphere (e.g., through reactions between the $X^{\bullet}$ and $OH^{\bullet}$ radicals), and that the species including a halogen element are crucial for most of the ozone removal processes, the title complexes in the present study are of great potential interest in the field of atmospheric chemistry relevant to ecological aspects. These particular dimers considered in the present paper may potentially act as chaperones and may act to enhance formation of dimers relevant to ozone removal processes, similar to the case of radical complexes involving H_2O. In the present study, we also consider the importance of cooperative effects when larger intermolecular clusters of the form $(HOX)_2$···SO_3 are formed. The conclusions derived with respect to these aspects may be potentially rather helpful for modeling the kinetics of atmospheric processes, which is one of the key aspects in ozone depletion process.

Recently theoretical studies of noncovalently bonded complexes of SO_3 with HX (X = F, Cl, Br),[11] CH_3X (X = F, Cl, Br),[12] HO_2,[13] CO_2,[14] HCN and CH_3CN,[15] H_2O[16] and $(H_2O)_{n=1-3}$,[17] NH_3[18] and $NH_{3-n}X_n$ (n = 0−3; X = F, Cl),[19] and C_5H_5N[20] have been reported in the literature. To the best of our knowledge, the formation of the complex of sulfur trioxide with HOX (X = F, Cl, Br) has not yet been determined theoretically or experimentally. This has motivated search for the structure and stability of the complexes formed as a result of the bonding between a strong Lewis acid such as SO_3 and strong oxyacids HOX (X = F, Cl, Br) for the first time. Besides the standard explorations of the SO_3···HOX (X = F, Cl, Br) potential energy hypersurfaces at various levels of theory, we also provide relatively highly accurate data for the *anharmonic* O−H vibrational frequency shifts upon SO_3···HOX (X = F, Cl, Br)

* Corresponding author: m-solimannejad@araku.ac.ir.

10.1021/jp047323s CCC: $30.25 © 2005 American Chemical Society
Published on Web 01/20/2005

dimer formation. In particular, these data should be very helpful in designing and performing the potential experimental studies of this dimer, and the interpretation of the corresponding experimental spectroscopic data. We also analyze the electron density of the minima located on various $SO_3\cdots HOX$ (X = F, Cl, Br) dimers PESs employing Bader's AIM methodology,[21] as well as the NBO approach.[22]

Computational Details

Quantum chemical calculations were employed to obtain the geometries of the monomers and complex corresponding to the minima on the considered MP2 potential energy surfaces (PESs). We fully optimized all structures using tight convergence criteria with the second-order Møller−Plesset perturbation theory (MP2) method with various basis sets, ranging from MP2/6-31G(d) to MP2/6-311++G(3df,3pd). Schlegel's gradient optimization algorithm[23] was used in all productive searches for the minima on the considered PESs. No symmetry constraints were imposed during the optimization process. However, since the optimized structures of the complex corresponded to C_s symmetry at all levels of theory, for some particular cases (when the apparent symmetry was C_1, but obviously rather close to C_s) it was necessary to do the reoptimization within the higher symmetry. For each such case, the higher-symmetry geometry corresponded to lower energy. All the results presented below for the dimers, therefore, correspond to species with C_s symmetry (the corresponding electronic state being $^1A'$). Our first set of calculations was focused on the optimization of the structures with small basis sets, but we subsequently performed optimizations with much larger, up to 6-311++G (3df,3pd) basis set(s) to reduce the basis set superposition error (BSSE) as much as possible. The larger basis sets produced a counterpoise correction that is small, and that is not likely to make a significant difference in the final computed binding energies at MP2 level of theory. Zero-point energy (ZPE) corrections were calculated using the harmonic frequencies at the G3 level of theory for HOF and HOCl complexes and G2 level for HOBr complexes, due to the enormous computational resources needed for MP2/6-311++G (3df,3pd) frequency calculations. Besides applying the previously mentioned MP2 methods with a series of successively increasing basis sets, we also provide a sort of benchmark testing in the present study, by comparing the MP2 energetical data with the G2- and G3-derived reference ones, which we also calculate in this study.

Calculation of the Anharmonic Vibrational Frequencies and IR Intensities. The *anharmonic* O−H stretching frequencies for the O−H oscillators within the free XOH systems and also for the (X)O−H$\cdots$OSO$_2$ hydrogen bonded oscillators within the studied dimer of XOH with SO_3 were calculated in the following manner. To obtain each vibrational potential energy curve ($V = f(r_{OH})$), series of 15 pointwise energy calculations were performed in the case of all O−H oscillators, varying the O−H distances from 0.85 to 1.55 Å. Subsequently, the obtained energies were least-squares fitted to a fifth order polynomial in r_{OH}, the potential energy functions afterward cut after fourth order and transformed into Simons−Parr−Finlan (SPF) type coordinates $\rho = 1 - r_{OH,e}/r_{OH}$[24] (where $r_{OH,e}$ is the equilibrium value). The resulting one-dimensional vibrational Schrödinger equation was solved variationally using 15 harmonic oscillator eigenfunctions as a basis. Superiority of the SPF-type coordinates over the "ordinary" bond stretch ones when variational solution of the vibrational Schrödinger equation is in question has been well established. These particular coordinates (in comparison to the standard bond-stretch ones) allow for a faster convergence (with the number of basis functions used) and a greatly extended region of convergence of Hamiltonian matrix eigenvalues. The fundamental *anharmonic* O−H stretching frequencies were computed from energy differences between the ground and first excited vibrational states, while the anharmonicity constants (X) were computed from the equation

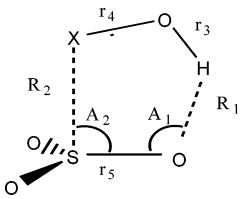

Figure 1. Definition of the geometrical parameters of HOX$\cdots$SO$_3$ (X = F, Cl, Br) complexes with C_s symmetry.

$$\tilde{\nu}_{OH} = \omega_{0,OH} + 2X \quad (1)$$

In the previous equation, $\omega_{0,OH}$ is the harmonic eigenvalue (obtained from the harmonic force constant k_2).

The IR intensities were calculated within the electrical harmonic approximation according to the following relation

$$A_s = \frac{1}{4\pi\epsilon_0}\frac{N_A\pi}{3c^2 m_H}\cdot\left(\frac{\partial\mu}{\partial r_{OH}}\right)^2_{rOH,e} \quad (2)$$

where A_s is the molar absorption coefficient (expressed in km mol^{-1} when $\partial\mu/\partial r_{OH}$ is expressed in D/Å) while m_H is the vibrating proton mass. The squared dipole moment derivatives are defined by

$$\left(\frac{\partial\mu}{\partial r_{OH}}\right)^2_{r_{OH,e}} = \left(\frac{\partial\mu_x}{\partial r_{OH}}\right)^2_{r_{OH,e}} + \left(\frac{\partial\mu_y}{\partial r_{OH}}\right)^2_{r_{OH,e}} + \left(\frac{\partial\mu_z}{\partial r_{OH}}\right)^2_{r_{OH,e}} \quad (3)$$

Each of the derivatives on the right-hand side of eq 3 was computed by a fourth-order polynomial interpolation of the corresponding function $\mu_i(r_{OH})$ and subsequent differentiation at $r_{OH,e}$.

All calculations were performed with the Gaussian98 series of programs.[25]

Results and Discussion

Geometries, Interaction Energies, and Thermochemical Stabilities. The minimum located on MP2 PESs of the HOX$\cdots$SO$_3$ complexes considered in this study is schematically presented in Figure 1. All the minima on the considered MP2 PESs are characterized with C_s symmetry, the corresponding electronic state being $^1A'$. As can be seen from Figure 1, HOX is bounded to SO_3 via the interaction between the lone pair on halogen with the sulfur atom, and also through formation of hydrogen bond between HOX hydrogen atom and one of the SO_3 oxygen atoms. The calculated structural parameters at different theoretical levels are shown in Table 1.

The calculated binding energies (given in kcal mol^{-1}) for HOX−SO$_3$(g) → HOX(g) + SO$_3$(g) at different levels are shown in Table 2. Our calculations reveal stabilization energies of 5.43, 6.02, and 5.98 kcal mol^{-1} at the MP2/6-311++G(3df,3pd) level, for HOF$\cdots$SO$_3$, HOCl$\cdots$SO$_3$, and HOBr$\cdots$SO$_3$ complexes, respectively. This observation implies that HOX$\cdots$SO$_3$ (X = F, Cl, Br) complexes should be experimentally observable in the gas phase. However, since this implication is based purely on the interaction energy data, we have also calculated the relevant thermochemical parameters, which should be much more relevant for eventual experimental

TABLE 1: Structural Parameters Calculated for HOX−SO_3 (X = F, Cl, Br) Complexes at Different Level[a]

level of theory	R_1	R_2	r_3	r_4	r_5	A_1	A_2
			HOF···SO_3				
MP2/6-31G(d)	2.026	2.650	0.984	1.449	1.464	108.6	81.4
MP2/6-311++G(d,p)	2.033	2.839	0.973	1.433	1.453	116.4	75.8
MP2/6-311++G(2df,2p)	2.061	2.700	0.972	1.426	1.440	108.0	81.0
MP2/6-311++G(3df,3pd)	2.053	2.675	0.971	1.424	1.434	108.5	81.6
			HOCl···SO_3				
MP2/6-31G(d)	2.059	3.218	0.982	1.712	1.464	116.9	76.1
MP2/6-311++G(d,p)	2.042	3.320	0.970	1.711	1.453	122.7	72.9
MP2/6-311++G (2df,2p)	2.036	2.957	0.972	1.687	1.440	111.8	83.1
MP2/6-311++G (3df,3pd)	2.038	3.003	0.971	1.680	1.434	112.8	82.1
			HOBr···SO_3				
MP2/6-31G(d)	2.069	3.239	0.984	1.859	1.464	117.6	79.5
MP2/6-311++G(d,p)	2.049	3.405	0.971	1.854	1.453	123.0	80.7
MP2/6-311++G(2df,2p)	2.064	3.079	0.972	1.820	1.440	113.8	70.6
MP2/6-311++G(3df,3pd)	2.066	3.109	0.971	1.821	1.434	114.4	71.4

[a] Distances are in angstroms and angles are in degrees (see Figure 1).

TABLE 2: Binding Energies (kcal mol^{-1}) Calculated for HOX−SO_3(g) → HOX(g) + SO_3(g) at Different Levels

level of theory	D_e	D_0
HOF···SO_3		
MP2/6-31G(d)	7.66	6.78
MP2/6-311++G(d,p)	5.69	4.81
MP2/6-311++G(2df,2p)	4.95	4.07
MP2/6-311++G(3df,3pd)	5.43	4.55
G3	4.45	3.57
HOCl···SO_3		
MP2/6-31G(d)	5.22	4.16
MP2/6-311++G(d,p)	5.44	4.37
MP2/6-311++G (2df,2p)	5.50	4.43
MP2/6-311++G(3df,3pd)	6.02	4.95
G3	5.69	4.62
HOBr···SO_3		
MP2/6-31G(d)	7.72	6.69
MP2/6-311++G(d,p)	5.43	4.40
MP2/6-311++G(2df,2p)	5.80	4.77
MP2/6-311++G(3df,3pd)	5.98	4.95
G2	4.90	3.87

detection of the complex in question. Standard statistical mechanics approaches were employed to calculate thermochemical parameters at both 0 and 298 K, which is a temperature relevant to atmospheric processes. The G3 approach gives values of −4.45, −5.04, 3.25, and −5.69, −5.21, and 1.66 kcal mol^{-1} for the interaction energy at 0 K, $\Delta H°$, and ΔG(298 K) of the HOF···SO_3 and HOCl···SO_3 complexes, respectively. The corresponding data employing the G2 approach are −4.90, −4.46 and −3.39 kcal mol^{-1} for the interaction energy, $\Delta H°$, and ΔG(298 K) of the HOBr···SO_3 complex. These parameters further support the possibility for the existence (and therefore also for experimental detection) of these dimers at temperature lower than room temperature.

Intuitively, the minima depicted in Figure 1 should be expected to be of greatest stability on the considered PESs (as they are stabilized by both H-bonding and an additional S···X noncovalent interaction). It is, however, interesting to make further, at least preliminary explorations of other regions of the studied PESs, to detect the other possible minima. The existence of such minima could in principle allow derivation of conclusions on the relative importance of H-bonding interaction vs the X···S noncovalent interaction. We have therefore carefully performed a series of explorations of various regions of the MP2/6-31G(d) PESs of the title 1:1 complexes, employing the GDIIS algorithm in the search for additional minima. This algorithm was implemented due to the rather flat character of other regions of the studied PESs. Indeed, additional minima were located for all complexes considered, which are depicted in Figure 2. As can be seen, these minima are characterized by an O···S contact, while the H-bonding interaction seems to be of much less importance for their stability. It is worth noting that, besides the other factors, purely electrostatic interaction, especially the dipole−quadrupole term should be expected to stabilize these structures as well, as may be easily inferred from elementary electrostatic considerations. The interaction energies for these minima (at MP2/6-31G(d) level of theory, not including the ZPVE corrections) are 7.40, 9.12, and 12.67 kcal mol^{-1} for SO_3···HOF, SO_3···HOCl, and SO_3···HOBr, respectively. It follows from the previous energy data that the stability of these minima is quite comparable to the stability of minima with the structure as depicted in Figure 1. This is not surprising, since the additional minima are also characterized by H-bonding interaction, besides the O···S contact. We will devote a separate paper to a more detailed study of the complete PES of the studied dimer.

As the considered noncovalently bonded molecular complexes are of certain importance for atmospheric chemistry (as ex-

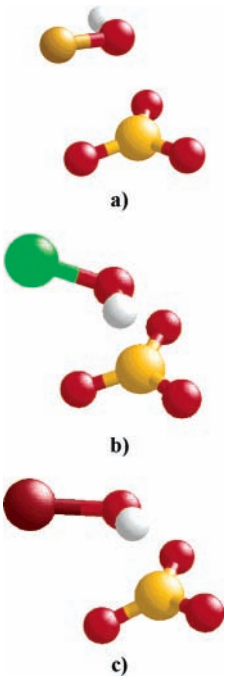

Figure 2. Additional minima located on the MP2/6-31G(d,p) PESs of the studied SO_3···HOF (a), SO_3···HOCl (b), and SO_3···HOBr (c) complexes.

plained in detail in the Introduction), some additional insights into the dynamics of their formation were considered in the present study. Thus, the importance of cooperative effects in such intermolecular bonding were examined by considering a bit larger clusters of the type $(HOX)_2\cdots SO_3$. The MP2/6-31G(d) PESs of the $(HOX)_2\cdots SO_3$ clusters were therefore also explored. The located minima at the mentioned PESs are presented in Figure 3. It is interesting to note that the additional HOX molecule does not bind in an identical way to the SO_3 system as does the first one in the case of all clusters considered. Since it was not our intention in the present study to explore the complete PESs of the 2:1 clusters, we will briefly refer in this context only to the single minimum located, taking the structures analogous as the one for $(HOF)_2\cdots SO_3$ cluster, depicted in Figure 3a as a starting point for the minima-search on the PESs. Following the standard notation, the total energy E_n of an n-body cluster may be represented as a sum of the one-, two-, three-, four-, etc. body terms in the following way:

$$E_n = \sum_{i=1}^{n} E(i) + \sum_{i=1}^{n-1}\sum_{j>i}^{n} \Delta^2 E(ij) + \sum_{i=1}^{n-2}\sum_{j>i}^{n-1}\sum_{k>j}^{n} \Delta^3 E(ijk) + \sum_{i=1}^{n-3}\sum_{j>i}^{n-2}\sum_{k>j}^{n-1}\sum_{l>k}^{n} \Delta^4 E(ijkl) + \ldots$$

where

$$\Delta^2 E(ij) = E(ij) - \{E(i) + E(j)\}$$

$$\Delta^3 E(ijk) = E(ijk) - \{E(i) + E(j) + E(k)\} - \{\Delta^2 E(ij) + \Delta^2 E(ik) + \Delta^2 E(jk)\}$$

etc., following the same logic.

The total binding energies in the case of minima depicted in Figure 3 are 15.36, 14.63, and 15.35 kcal mol^{-1} for $SO_3\cdots(HOF)_2$, $SO_3\cdots(HOCl)_2$, and $SO_3\cdots(HOBr)_2$ respectively. The two-body contributions are by far the most predominant ones in the overall interaction energies for all of the studied 2:1 complexes—the exact numerical values being 14.61, 14.37, and 15.32 kcal mol^{-1} for $SO_3\cdots(HOF)_2$, $SO_3\cdots(HOCl)_2$, and $SO_3\cdots(HOBr)_2$ respectively. Third-body terms contribute to the total interaction energies only by 0.76, 0.26, and 0.04 kcal mol^{-1} in the case of $SO_3\cdots(HOF)_2$, $SO_3\cdots(HOCl)_2$, and $SO_3\cdots(HOBr)_2$ respectively.

Anharmonic O−H Vibrational Frequencies and IR Intensities. The calculated anharmonic O−H stretching vibrational frequencies for free XOH species, as well as for the hydrogen-bonded dimers of XOH with SO_3 at the MP2/6-311++G(2df,2p) level of theory together with the corresponding harmonic eigenvalues, anharmonicity constants, and IR intensities, are given in Table 3. In Table 4, on the other hand, the O−H stretching vibrational potential parameters obtained by least-squares fifth-order polynomial fitting to the MP2 energies are given. As can be concluded from the results presented in these two tables, the O−H stretching frequency downshifts upon H-bonding interaction of XOH species with the considered inorganic SO_3 proton acceptor fall in the range from 80 to 100 cm^{-1}. These frequency downshifts are accompanied by rather modest changes in the corresponding vibrational anharmonicities with respect to the corresponding free species. The IR intensities of the OH modes increase by approximately a factor of 2 upon hydrogen bonding in all of the studied systems. All these characteristics imply that the currently studied intermolecular hydrogen bonding interactions may be classified as hydrogen bonds of moderate strength. The possible coupling of the high-frequency O−H stretching mode with the lower-frequency "hydrogen bond vibration" of the O···O type (which is not accounted for in the present 1D vibrational potential calculations) is expected to be small in the case of weak to moderate strength hydrogen bonds, so the anharmonic vibrational fre-

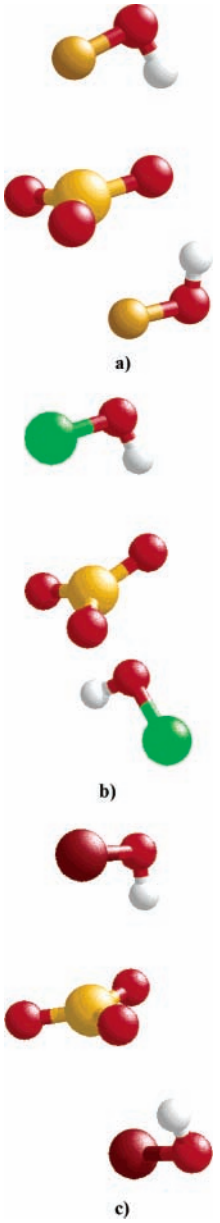

Figure 3. Minima located on the MP2/6-31G(d,p) PESs of the studied $SO_3\cdots(HOF)_2$ (a), $SO_3\cdots(HOCl)_2$ (b), and $SO_3\cdots(HOBr)_2$ (c) complexes.

TABLE 3: Calculated *Anharmonic* Vibrational Frequencies for Monomeric HOX and Dimeric $HOX\cdots SO_3$ (X = F, Cl, Br) Hydrogen Bonded Oscillators, together with the Corresponding Harmonic Eigenvalues, Anharmonicity Constants, and IR Intensities at MP2/6-311++G(2df,2p) Level and the Anharmonic Vibrational Frequency Shifts with Respect to the Free Monomeric Units

	$r_{OH,e}$/ Å	ν/ cm^{-1}	$\Delta\nu$/ cm^{-1}	ω_0/ cm^{-1}	-X/ cm^{-1}	I/(km mol^{-1})
HOF	0.9683	3609.9		3795.5	92.8	52.68
HOCl	0.9670	3618.9		3805.6	93.4	83.90
HOBr	0.9675	3615.1		3800.9	92.9	91.13
$HOF\cdots SO_3$	0.9731	3532.5	−77.4	3726.1	96.8	133.04
$HOCl\cdots SO_3$	0.9727	3518.7	−100.2	3717.7	99.5	146.46
$HOBr\cdots SO_3$	0.9727	3523.4	−91.7	3720.7	98.7	134.53

TABLE 4: Calculated Vibrational Potential Parameters for Monomeric O−H and Dimeric O−H···O Hydrogen Bonded Oscillators in the Case of the Studied Complex of HOX with SO_3

	k_2/(mdyn Å^{-1})	k_3/(mdyn Å^{-2})	k_4/(mdyn Å^{-3})	k_5/(mdyn Å^{-4})
HOF	4.0510	−8.914	10.22	−5.1
HOCl	4.0727	−8.970	10.24	−5.1
HOBr	4.0627	−8.939	10.23	−5.1
HOF···SO_3	3.9042	−8.739	10.11	−5.1
HOCl···SO_3	3.8867	−8.767	10.06	−5.0
HOBr···SO_3	3.8930	−8.754	10.04	−5.0

quency shifts calculated in the present study are expected to be of valuable help in designing and performing the experimental spectroscopic studies of the systems in question, as already demonstrated in our previous studies.[6,10,13,26]

The previously outlined data should be very valuable for the future experimental studies of the dimeric species considered in this study. However, the other vibrational modes, especially the intermolecular ones, should be expected to be much less anharmonic than the O−H vibrations. To provide further theoretical support for the future spectroscopic experiments, in Table 5, the harmonic vibrational frequencies for free HOX species, as well as for the dimeric SO_3···HOX ones, are presented. Except for the modes which are mostly affected by the H-bonding interaction, the vibrational frequency shifts of all other modes are rather modest, as can be seen from this Table 5.

Bader AIM Analysis. To further characterize the noncovalent interaction of H-bonding type in the studied dimers of HOX species with SO_3, several basic parameters arising from Bader's theory of atoms in molecules (AIM)[21] were calculated. Bader analysis of the electron density of the XOH···OSO_2 complexes included the search for the (3,−1) i.e. bond critical points (BCPs), calculation of the charge densities $\rho(r_c)$ and the corresponding density laplacians $\nabla^2\rho(r_c)$ at (3,−1) BCPs, and the corresponding ellipticities. To confirm the presence of a hydrogen bond between two molecular systems within Bader's theory, the electron density gradient vector field topology has to be investigated. Of central importance within this context is the existence of bond critical points corresponding to intermolecular X−H···Y contacts and also their quantitative characteristics. The critical point is a point characterized with $\nabla\rho(r_c) = 0$. The curvature of the electronic density at the critical point, on the other hand, is characterized by the value of the corresponding laplacian, i.e. $\nabla^2\rho(r_c)$ (the 3 × 3 Hessian matrix of the second partial derivatives with respect to coordinates). If we denote the three eigenvalues of the $\nabla^2\rho(r)$ Hessian matrix by λ_1, λ_2 and λ_3 (denoted in such a way that $\lambda_1 < \lambda_2 < \lambda_3$, λ_3 being set along the internuclear vector), then the actual $\nabla^2\rho(r_c)$ value is calculated as the trace of the Hessian matrix:

$$\nabla^2\rho(r_c) = \sum_{i=1}^{3}\lambda_i$$

Within this notation, the ellipticity associated with a chemical bond is defined with

$$\epsilon = \frac{\lambda_1}{\lambda_2} - 1$$

The values for all the relevant AIM quantities (calculated at MP2/6-311++G(2df,2p)//MP2/6-311++G(2df,2p) level of theory) corresponding to the BCPs characterizing the intermolecular (X)O−H···O(SO_2) as well as the (HO)X···S(O_3) contacts, as well as those corresponding to the intramolecular O−H BCP within the XOH species, are given in Table 6. As can be seen, the BCPs corresponding to the intermolecular (X)O−H···O(SO_2) contacts in which the XOH species play the role of a proton donor are characterized by small $\rho(r_c)$ values and $\nabla^2\rho(r_c) > 0$ (implying typical interactions of the "*closed-shell*" type). These data indicate that the electronic charge is locally depleted at the intermolecular BCPs, the kinetic energy $G(r)$ being in local excess over the value determined by the average virial ratio. According to the actual $\rho(r_c)$ and $\nabla^2\rho(r_c)$ values at this particular intermolecular (3,−1) BCP, applying the proposed AIM-based criteria for hydrogen bonding,[21] the present hydrogen bonds may be classified as moderate strength ones, which is in line with the corresponding conclusion arising from the analysis of the anharmonic OH stretching vibrational frequency shifts outlined before in this paper. The hydrogen bond strength is also revealed by a comparison of the $\rho(r_c)$ and $\nabla^2\rho(r_c)$ values corresponding to the intramolecular (3,−1) BCP (the BCP corresponding to the "*shared*" O−H interaction) in the case of free XOH species and in the case of hydrogen bonded dimers of XOH with SO_3, indicating a $\rho(r_c)$ (and $|\nabla^2\rho(r_c)|$) value decreases at the O−H BCP upon hydrogen bonds formation. As can be seen from Table 6, the ellipticities of the O−H bonds within the HOX systems decrease upon dimer formation, indicating a decrease in the stabilities of these bonds.

The additional existing intermolecular contacts within the studied dimers are of a (HO)X···S(O_3) type, the BCP corresponding to these contacts being again characterized by small $\rho(r_c)$ values and $\nabla^2\rho(r_c) > 0$. These data also indicate the noncovalent type of the interactions in question.

TABLE 5: Harmonic Vibrational Frequencies for Monomeric HOX and SO_3 as Well as for the Corresponding Dimeric Species Calculated at MP2/6-31G(d) Level of Theory (with Only the Most Relevant Vibrational Modes for This Interaction Shown)

mode	free HOF	free HOCl	free HOBr	free SO_3	HOF···SO_3	HOCl···SO_3	HOBr···SO_3
ν(OH)	3711.9	3712.7	3697.4		3644.2	3661.2	3642.0
δ(HOX)	1402.4	1320.6	1230.8		1471.0		1284.0
ν_{as}(SO_3)				1394.5	1414.8	1409.5	1409.7
ν_{as}(SO_3) + δ(HOX)						1397.1	1384.1
ν_{as}(SO_3) + δ(HOX)						1366.2	
ν_{as}(SO_3)				1394.5	1377.0		
ν_{s}(SO_3)				1020.1	1026.4	1023.4	1025.0
ν(O−F)	984.3				984.2		
ν(O−Cl)		756.3				758.4	
ν(O−Br)			628.9				635.1
δ(SO_3)				497.6	500.3	497.6	498.0
τ(OH) + δ(SO_3)						497.1	497.1
δ(SO_3)				497.6	499.1		
γ(SO_3)				458.7	462.4	455.7	448.6
τ(OH)					301.0	283.3	273.5

TABLE 6: Results from the AIM Analysis of the Relevant (3,−1) BCPs of the Free HOX as Well as for the Studied SO_3 Complexes with HOX (X = F, Cl, Br)[a]

BCP	$\rho(r_c)$	$\nabla^2\rho(r_c)$	ϵ
	Free XOH		
(F)O−H	0.3694	−2.817	0.046
(Cl)O−H	0.3656	−2.745	0.030
(Br)O−H	0.3636	−2.706	0.027
	XOH−SO_3		
(F)O−H	0.3633	−2.796	0.044
(Cl)O−H	0.3574	−2.709	0.029
(Br)O−H	0.3563	−2.679	0.026
(FO)H···O(SO_2)	0.0178	0.069	0.010
(ClO)H···O(SO_2)	0.0189	0.072	0.021
(BrO)H···O(SO_2)	0.0179	0.068	0.035
(HO)F···S(O_3)	0.0176	0.061	0.376
(HO)Cl···S(O_3)	0.0206	0.056	0.166
(HO)Br···S(O_3)	0.0205	0.046	0.148

[a] All values are in atomic units; all calculations were performed with the 6-311++G(2df,2p) basis set.

NBO Analysis. Natural bond orbital (NBO) analysis[22] was also performed for the minima found on the studied HOX−SO_3, PESs, to derive conclusions about the direction and magnitude of the charge-transfer (CT) interactions. For these purposes, a second-order perturbation theory (SOPT) analysis of the Fock matrix within the NBO basis was carried out. The results from this analysis (at HF/6-311++G(2df,2p)//MP2/6-311++G(2df,2p) level of theory) for the minima on the corresponding PESs are summarized in Table 7.

As can be seen from Table 7, the CT between the monomeric units occurs in both directions, from the proton-accepting to the proton-donating unit and vice versa. The most relevant contribution (in energetic sense) to the proton-acceptor → proton-donor CT occurs from the proton-acceptor n′(O) and n″(O) orbitals to the proton-donor σ^*(O−H) orbital. However, also quite significant CT occurs also from the proton-acceptor σ^*(S−O) orbital to the proton-donor σ^*(O−H) orbital. The last contribution is in fact the most significant in the sense of absolute quantity of the transferred charge, although its energetic importance is much less. When the proton-donor → proton-acceptor CT is in question, the most significant interaction contributing to it is the n(X) → σ^*(S−O) one.

In a quantitative sense, the energetic effects due to these interactions may be estimated by the second-order perturbation theoretical expressions of the form:[22]

$$\Delta E^{(2)}_{\psi_{\text{donor}}\rightarrow\psi_{\text{acceptor}}} \approx -2\cdot\frac{\langle\psi^*_{\text{don}}|\hat{F}|\psi_{\text{acc}}\rangle^2}{\epsilon_{\text{acc}}-\epsilon_{\text{don}}}$$

where ϵ_i is a diagonal NBO matrix element of the Fock operator $\hat{F}$. The quantities of transferred charge from a given donor to a given acceptor orbital may be estimated again using elementary perturbation theory arguments, leading to the following approximate formula:[22]

$$q_{\psi_{\text{donor}}\rightarrow\psi_{\text{acceptor}}} \approx 2\left(\frac{\langle\psi^*_{\text{don}}|\hat{F}|\psi_{\text{acc}}\rangle}{\epsilon_{\text{acc}}-\epsilon_{\text{don}}}\right)^2$$

All the NBO parameters related to the outlined discussion are presented in Table 7. Although being rather small (on an absolute scale), the CT is of chemical significance in the present case, as has been often found for a variety of analogous interacting systems.[6,9,10,26]

Conclusion

A high-level theoretical evidence for the possibility of the existence and stability of dimers between HOX (where X is F, Cl or Br) species and SO_3 systems potentially relevant to atmospheric chemistry is presented in this paper. A detailed analysis regarding the thermochemistry of formation and the electronic density as well as the stability of these complexes is performed at various theoretical levels. The *anharmonic* OH stretching vibrational frequency shifts of the HOX species upon dimer formation are also presented, which are expected to be of valuable help in designing and performing experiments for identification of the studied species. Bader (AIM) and NBO analyses of the electron density of the title complexes were also carried out. The results of the present theoretical study predict that the noncovalently bonded species considered should be thermodynamically stable and also spectroscopically detectable. High level quantum chemical calculations performed to make reliable predictions of the *anharmonic* vibrational frequency shifts of the O−H modes upon dimer formations enable easier interpretation of experimental data when they became available.

TABLE 7: Results from the Second-Order Perturbation Theory Analysis Analog of the Fock Matrix within the NBO Basis for the HOX−SO_3 Complexes at the MP2/6-311++G(2df,2p) Level of Theory

donor orbital	acceptor orbital	$\Delta E^{(2)}$/(kJ mol^{-1})	$(\epsilon_{\text{acc}}-\epsilon_{\text{don}})$/a.u.	$\langle\psi^*_{\text{don}}\|F\|\psi_{\text{acc}}\rangle$/a.u.	$q_{\text{donor}\rightarrow\text{acceptor}}/e$
		HOF			
n′(O_{SO_3})	σ^*(O−H)	2.97	1.15	0.056	0.005
n″(O_{SO_3})	σ^*(O−H)	1.20	1.82	0.042	0.001
σ^*(S−O)	σ^*(O−H)	0.43	0.11	0.025	0.103
n(F)	σ^*(S−O)	0.95	1.20	0.032	0.001
n(F)	σ^*(S−O)	0.95	1.20	0.032	0.001
		HOCl			
n′(O_{SO_3})	σ^*(O−H)	3.00	1.17	0.057	0.005
n″(O_{SO_3})	σ^*(O−H)	1.36	1.84	0.045	0.001
$\sigma^{*\prime}$(S−O)	σ^*(O−H)	0.44	0.13	0.027	0.086
n(Cl)	$\sigma^{*\prime}$(S−O)	2.81	0.95	0.048	0.005
n(Cl)	$\sigma^{*\prime}$(S−O)	2.81	0.95	0.048	0.005
n(Cl)	*Ry**(S)	1.93	1.54	0.049	0.002
n(Cl)	$\sigma^{*\prime\prime}$(S−O)	0.65	1.07	0.024	0.001
		HOBr			
n′(O_{SO_3})	σ^*(O−H)	2.54	1.19	0.053	0.004
n″(O_{SO_3})	σ^*(O−H)	1.15	1.85	0.041	0.001
$\sigma^{*\prime}$(S−O)	σ^*(O−H)	0.39	0.15	0.027	0.065
n(Br)	$\sigma^{*\prime\prime}$(S−O)	3.14	0.90	0.050	0.006
n(Br)	$\sigma^{*\prime\prime}$(S−O)	3.14	0.90	0.050	0.006

All these considerations strongly encourage performing of a matrix isolation study of the title complexes in the future as well.

References and Notes

(1) Müller-Dethlefs, K.; Hobza, P. *Chem. Rev.* **2000**, *100*, 143.
(2) Molina, L. T.; Molina, M. J. *J. Phys. Chem.* **1987**, *91*, 433.
(3) Molina, M. J. *Science* **1987**, *238*, 1253.
(4) Cox, R. A.; Hayman, G. D. *Nature* **1988**, *332*, 796.
(5) Sander, S. P.; Friedl, R. R.; Yung, Y. L. *Science* **1989**, *245*, 1095.
(6) Solimannejad, M.; Pejov, Lj. *Chem. Phys. Lett.* **2004**, *385*, 394.
(7) Solimannejad, M.; Boutalib, A. *Chem. Phys. Lett.* **2004**, *389*, 359.
(8) Solimannejad, M.; Boutalib, A. *J. Phys. Chem. A* **2004**, *108*, 4769.
(9) Pejov, Lj.; Hermansson, K. *J. Chem. Phys.* **2003**, *119*, 313.
(10) Pejov, Lj. *Chem. Phys.* **2002**, *285*, 177.
(11) Chaoo, J.; Kim, S.; Kwon, Y. *Chem. Phys. Lett.* **2002**, *358*, 121.
(12) Solimannejad, M.; Tahmassebi, D.; Alikhani, M. E. *Spectrochim. Acta Part A* **2005**, *61*, 373.
(13) Solimannejad, M.; Azimi, G.; Pejov, Lj. *Chem. Phys. Lett.* **2004**, *391*, 201.
(14) Givan, A.; Loewenschuss, A.; Nielsen, C. J. *J. Mol. Struct.* **2002**, *604*, 147.
(15) Burns, W. A.; Phillips, J. A.; Canagaratna, M.; Goodfriend, H.; Leopold, K. R. *J. Phys. Chem. A* **1999**, *103*, 7445.
(16) Hofmann, M.; Schleyer, P. von Rague. *J. Am. Chem. Soc.* **1994**, *116*, 4947.
(17) Standard, J. M.; Buckner, I. S.; Pulsifer, D. H. *J. Mol. Struct.* (*THEOCHEM*) **2004**, *673*, 1.
(18) Canagaratna, M.; Phillips, J. A.; Goodfriend, H.; Leopold, K. R. *J. Am. Chem. Soc.* **1996**, *118*, 5290.
(19) Solimannejad, M.; Boutalib, A. *J. Phys. Chem. A* **2004**, *108*, 10342.
(20) Hunt, W.; Leopold, K. R. *J. Phys. Chem. A* **2001**, *105*, 5498.
(21) Bader, R. F. W. *Chem. Rev.* **1991**, *91*, 893 and references therein.
(22) Reed, A. E.; Curtiss, L. A.; Weinhold, F. *Chem. Rev.* **1988**, *88*, 269 and references therein.
(23) Schlegel, H. B. *J. Comput. Chem.* **1982**, *3*, 214.
(24) Simons, G.; Parr, R. G.; Finlan, J. M. *J. Chem. Phys.* **1973**, *59*, 3229.
(25) Frisch, M. J.; Trucks, G. W.; Schlegel, H. B.; Scuseria, G. E.; Robb, M. A.; Cheeseman, J. R.; Zakrzewski, V. G.; Montgomery, J. A.; Stratmann, R. E.; Burant, J. C.; Dapprich, S.; Millam, J. M.; Daniels, A. D.; Kudin, K. N.; Strain, M. C.; Farkas, O.; Tomasi, J.; Barone, V.; Cossi, M.; Cammi, R.; Mennucci, B.; Pomelli, C.; Adamo, C.; Clifford, S.; Ochterski, J.; Petersson, G. A.; Ayala, P. Y.; Cui, Q.; Morokuma, K.; Malick, D. K.; Rabuck, A. D.; Raghavachari, K.; Foresman, J. B.; Cioslowski, J.; Ortiz, J. V.; Stefanov, B. B.; Liu, G.; Liashenko, A.; Piskorz, P.; Komaromi, I.; Gomperts, R.; Martin, R. L.; Fox, D. J.; Keith, T.; Al-Laham, M. A.; Peng, C. Y.; Nanayakkara, A.; Gonzalez, C.; Challacombe, M.; Gill, P. M. W.; Johnson, B.; Chen, W.; Wong, M. W.; Andres, J. L.; Gonzalez, Head-Gordon, C. M.; Replogle, E. S.; Pople, J. A. Gaussian 98, Revision A. 6. Gaussian, Inc.: Pittsburgh, PA, 1998.
(26) Pejov, Lj. *Chem. Phys. Lett.* **2003**, *376*, 11.